Electron bremsstrahlung spectrum, 1–500 keV*

C. M. Lee, Lynn Kissel, and R. H. Pratt
Department of Physics, University of Pittsburgh, Pittsburgh, Pennsylvania, 15260

H. K. Tseng
Department of Physics, National Central University, Chung-Li, Taiwan, Republic of China

(Received 2 December 1975)

Numerical data are obtained for the electron bremsstrahlung energy spectrum resulting from incident electrons of kinetic energy 1–500 keV, under the assumption that the process is described as a single-electron transition in a relativistic self-consistent screened potential, using partial-wave expansions. Comparisons with simpler analytical approximations show that these are at best of qualitative validity in this energy range. Our data are used to construct more complete tables of the spectrum by interpolation.

I. INTRODUCTION

In recent years it has become possible to obtain fairly accurate theoretical predictions for properties of the bremsstrahlung radiation from incident electrons with kinetic energies in the range of keV.[1] This has coincided with increased needs for such results, as in radiation physics[2] and in controlled thermonuclear research.[3] Previous theoretical approaches[4-7] are, as we shall see, at best of qualitative validity in this energy range; a review of the theory, emphasizing the MeV region, has been given by Koch and Motz.[8]

Our calculations yield the electron bremsstrahlung energy spectrum, angular distributions, and polarization correlations for the process described as a single-electron transition in a relativistic self-consistent screened central potential V. Electron wave functions are obtained in partial-wave series by numerically integrating the radial Dirac equation; the radial integrals over radial wave functions are performed numerically and then summed numerically over the angular momentum variables. In our most recent work we have reported data for the energy spectrum at 50 keV[9] and for the tip limit of the spectrum[10,11] when the incident electron radiates almost all of its energy.

Here we wish to report rather complete data for the electron bremsstrahlung energy spectrum in the range of incident electron kinetic energies 1–500 keV. Our data, obtained for the Kohn-Sham[12] potential, are given in Sec. II together with some discussion of qualitative features of the spectrum. We have verified that, in this energy region, results are not sensitive to the detailed choice of self-consistent potential. However, for incident electron energies below 1 keV this choice, as well as many electron effects, becomes increasingly important. In Sec. III we compare our results with various simpler theoretical approximations, which we show are generally inadequate for quantitative purposes. In Sec. IV, we use our data to construct tables of the electron bremsstrahlung energy spectrum by interpolation; we believe that our interpolated values are accurate to at least 10%. We compare our values with existing experimental data and find satisfactory agreement.

II. NUMERICAL RESULTS

We present in Tables I–VI our numerical results for bremsstrahlung spectrum points $\sigma(k) \equiv \beta_1^2(k/Z^2)(d\sigma/dk)$, both for neutral [exact screened (ES)] and totally ionized [exact Coulomb (EC)] atoms. $\sigma(k)$ depends on three variables: the nuclear charge Z, the incident electron kinetic energy T_1, and the fraction of energy radiated k/T_1. We give data for six elements ($Z = 2$, 8, 13, 47, 79, and 92) at incident electron kinetic energies from 1 to 500 keV over the entire spectrum $k/T_1 = 0-1$. In each case the tables also show the value (EBF) obtained in the Born approximation[5] modified by the Elwert factor,[6] using the Thomas-Fermi-Molière form factor[13]; the ratios $\sigma_{\mathrm{EBF}}/\sigma_{\mathrm{ES}}$ are used for interpolation in constructing the tables of Sec. IV (EBF stands for the Elwert-factor Born-approximation form factor). The numerical results for $k/T_1 > 0$ were obtained from our partial-wave bremsstrahlung code previously described; the data for $k/T_1 \equiv 0$ were obtained from elastic scattering data using Low's low-energy theorem.[9,14] We have included in Table VII all our other numerical neutral spectrum data (except for tip-region points previously reported[1,10]), of which we have not made further use in this paper because we estimate it does not meet the same standard of accuracy, either due to an inadequate range of integration or inadequate number of partial waves. From comparison with values obtained by interpolation we will find that these data, which refer to

TABLE I. Bremsstrahlung data $\beta_1^2(k/Z^2)(d\sigma/dk)$ (in mb) for He ($Z=2$).

k/T_1 \ T_1	1 keV			5 keV			10 keV			50 keV			100 keV			500 keV		
	EC	ES	EBF	EC	ES	EBF	EC	ES	EBF	EC	ES	EBF	EC	ES	EBF	EC	ES	EBF
0.95		4.94	4.13		3.12	3.00		2.56	2.51		1.66	1.66		1.34	1.33		0.75	0.75
0.80	5.31	5.13	4.43		4.09	3.87		3.71	3.59		2.94	2.90		2.54	2.52		1.67	1.67
0.60		5.76	4.96		5.37	4.96		5.10	4.84		4.38	4.31		3.94	3.91		2.87	2.95
0.0		7.15	6.00		9.55	8.35		10.60	9.34		12.80	11.36		13.02	11.97		13.00	12.60

low-k/T_1 cases, were indeed accurate to within 5% except for 500 keV.

The factors $\beta_1^2(k/Z^2)$ are chosen to cancel the known dependence of $d\sigma/dk$ on these factors, resulting in a $\sigma(k)$ with a reduced magnitude of variation. $d\sigma/dk$ diverges with $1/k$ as $k \to 0$ (infrared divergence) due to the zero mass of the photon; $k(d\sigma/dk)$ is finite in this limit for a screened potential but still has a $-\ln k$ divergence in the point Coulomb case. (In either case the integrated energy-loss cross section $\int \sigma(k)\,dk$ is finite.) For high energies $\beta \cong 1$ and, in the Born approximation, $d\sigma/dk$ is proportional to Z^2; when $k/T_1 = 1$ and the Born approximation fails most badly, it is proportionate to Z^3, which is why $\sigma(k)$ is small for low Z at high energies. At low energies, except for small k/T_1, when $Z\alpha/\beta_1 \gg 1$ the Sommerfeld formula,[4,15] valid in the point Coulomb case, reduces to the classical Kramers result:

$$\frac{\beta_1^2 k}{Z^2}\frac{d\sigma}{dk} \cong \frac{16\pi}{3\sqrt{3}}\alpha^3 \cong 5.60 \text{ mb},$$

and shows the same dependence on k, β_1, and Z. However in the screened case the charge Z is increasingly shielded for low energies, and the tabulated $\sigma(k)$ drops; for a given energy the fractional shielding, and so the drop in $\sigma(k)$, increases with increasing Z.

For given Z and T_1, $\sigma(k)$ in the point Coulomb case starts from a finite value at the "tip" ($k/T_1 = 1$), gradually increases as k/T_1 decreases, and finally diverges logarithmically in the soft photon limit $k/T_1 \to 0$. The screened spectrum from a neutral atom lies below the point Coulomb spectrum. In the screened case $\sigma(k) = 0$ at the tip but rapidly rises in the first 5–50 eV; it remains finite in the soft photon limit. In both cases the spectrum becomes flatter with increasing Z for fixed T_1 and with decreasing T_1 for fixed Z, in accord with the condition $Z\alpha/\beta_1 \gg 1$ for the validity of the classical flat spectrum Kramers result. However with screening, $\sigma(k)$ at low energies has a maximum with decreasing k/T_1 and then decreases toward the soft-photon end of the spectrum. This screening effect sets in first for the higher Z's, at about 10 keV for Au ($Z=79$), 5 keV for Ag ($Z=47$), and 1 keV for Al ($Z=13$). For given k/T_1, screening is more important for small T_1; for given T_1, screening is more important for small k/T_1's — in both cases because smaller momentum transfers and larger distances are involved. The spectrum from a partially ionized atom lies between the point Coulomb and neutral atom cases.[16]

The tip region of the bremsstrahlung spectrum has rather special properties and has received separate study.[10,11] An approximate connection, for higher energies, with atomic photoeffect was

TABLE II. Bremsstrahlung data $\beta_1^2(k/Z^2)(d\sigma/dk)$ (in mb) for O ($Z=8$).

k/T_1 \ T_1	1 keV			5 keV			10 keV			100 keV			500 keV		
	EC	ES	EBF	EC	ES	EBF	EC	ES	EBF	EC	ES	EBF	EC	ES	EBF
0.99					5.49	5.12									
0.96					5.56	5.17									
0.95		4.86	4.75					5.21	4.81		2.31	2.19	0.99	0.98	0.95
0.90					5.71	5.25		5.22	4.90					1.29	1.25
0.80		4.91	4.84		5.93	5.42		5.45	5.13		3.17	3.07	1.86	1.86	1.81
0.60		5.01	4.95					6.14	5.74		4.42	4.26	3.06	3.04	3.04
0.50					6.73	6.09									
0.40								7.03	6.53						
0.00		4.82	4.68		7.61	6.98		8.74	7.97		11.60	10.74		12.20	11.64

first noted by Fano.[17] For very low energies resonance structures can develop in some cases.[11] And in the point Coulomb or partially-ionized-atom case a connection to radiative capture can be made via the quantum defect theory.[18] The data shown in this paper for $k/T_1=1$ have been obtained by extrapolation, not by direct calculation, and in the screened case should be understood as applying to some tens of eV back from the tip, as distinguished from the zero value which would be obtained precisely at the tip.

The low-frequency region of the spectrum also has special properties and has received separate study.[19] In this case, as discussed by Low,[14] the bremsstrahlung matrix element is related to the matrix element for elastic electron scattering. From this in the point Coulomb or partially ionized case the logarithmic divergence of the spectrum in the soft photon limit can be obtained analytically, while in the screened case the limit value is obtained as

$$\left(\frac{k}{Z^2}\frac{d\sigma_{\text{brem}}}{dk}\right)_{k=0}=\frac{4\alpha}{Z^2}\int_0^{\pi}\sin\theta\,d\theta\left(\frac{d\sigma}{d\Omega}\right)_{\text{elas}}\times[A(A^2-B^2)^{-1/2}\times\cosh^{-1}(A/B)-1], \quad (1)$$

Where $\beta_1=p_1/E_1$, $A=1-\beta_1^2\cos\theta$, $B=1-\beta_1^2$, with θ the electron scattering angle and $(d\sigma/d\Omega)_{\text{elas}}$ the differential elastic electron scattering cross section. The data of Tables I–VI for $k/T_1=0$ were obtained from elastic electron scattering data[20] in this way.

III. COMPARISON WITH APPROXIMATIONS

It is natural to ask to what extent and under what circumstances our numerical data confirm the validity of various simple approximations often used for the bremsstrahlung spectrum. To answer this question we present, in Tables VIII and IX, a comparison of some of our data with the predictions of simpler approximate calculations. In the following paragraph, we will briefly discuss these theories and our conclusions regarding their validity. We begin with the case of a point Coulomb potential, generally assumed in the simpler theories, then discuss screening, and finally comment on the energy-loss integral over the spectrum.

The classical bremsstrahlung radiation spectrum when an electron scatters from a point charge Z is discussed in textbooks.[21] For $\sigma(k)\equiv\beta_1^2(k/Z^2)(d\sigma/dk)$ one obtains

$$\sigma(k)=\frac{2\pi^2\alpha^3}{3}\frac{\nu_1 k}{T_1}iH^{(1)}_{i\nu_1 k/2T_1}(i\nu_1 k/2T_1)\times H^{(1)\prime}_{i\nu_1 k/2T_1}(i\nu_1 k/2T_1), \quad (2)$$

where $H^{(1)}$ and $H^{(1)\prime}$ are the Hankel function and its derivative, respectively, and ν_1 is defined as $Z\alpha/\beta_1$. Here the radiation reaction effects (i.e., change of classical orbit with electron energy loss by radiation) are neglected. Note that in this result the three variables, Z, T_1, and k/T_1 appear only in the single combination $\nu_1 k/2T_1$. Two important limiting situations are simple:

$$\sigma(k)\cong\frac{16\pi}{3\sqrt{3}}\alpha^3, \quad \frac{\nu_1 k}{2T_1}\gg 1 \quad (3)$$

$$\sigma(k)\cong\frac{16}{3}\alpha^3\ln\frac{2T_1}{\gamma\nu_1 k}, \quad \frac{\nu_1 k}{2T_1}\ll 1 \quad (4)$$

($\gamma=e^c$, where c is the Euler constant; $\gamma=1.7807\cdots$). At low energies Eq. (3) says that, except very close to the soft-photon end of the spectrum, the spectrum is flat and $\sigma(k)\cong 5.60$ mb. At our energies the condition $\nu_1 k/2T_1\gg 1$ is not yet satisfied; $\nu_1 k/2T_1=(0.683, 0.230)$, $(4.151, 1.377)$ for Al (5 and 10 keV) and Au (5 and 10 keV), respectively, but, qualitatively the spectrum is flattening with decreasing T_1 and comes within 20% of the classical constant value. The increase of $\sigma(k)$ associated with the logrithmic divergence, Eq. (3), is also clearly seen in our data. It should be noted that

TABLE III. Bremsstrahlung data $\beta_1^2(k/Z^2)(d\sigma/dk)$ (in mb) for Al ($Z=13$).

k/T_1 \ T_1	1 keV			5 keV			10 keV			50 keV			75 keV			100 keV			500 keV		
	EC	ES	EBF	EC	ES	EBF	EC	ES	EBF	EC	ES	EBF	EC	ES	EBF	EC	ES	EBF	EC	ES	EBF
0.99							5.82	5.53	5.25		3.90	3.72								0.96	0.90
0.95		4.15	4.50																		
0.90				6.25	5.58	5.43				4.17			3.58	3.55	3.39		3.16	3.00	1.48	1.47	1.38
0.80		4.06	4.56	6.45	5.70	5.58	6.21	5.81	5.58	4.56	4.48	4.31	4.03	4.00	3.82		3.64	3.46			
0.75																			2.34	2.33	2.19
0.60		3.95	4.60	7.00	5.98	5.91		6.23	6.03	5.55	5.42	5.20	5.12	5.06	4.81		4.75	4.51			
0.50				7.36	6.13														4.09	4.05	3.84
0.40				7.81	6.27	6.28	7.77	6.80	6.12	6.86	6.59	6.33									
0.00		3.62	4.23		6.63	6.51		7.80	7.49		10.30	9.61		10.7	10.04		11.10	10.30		11.90	11.29

TABLE IV. Bremsstrahlung data $\beta_1^2(k/Z^2)(d\sigma/dk)$ (in mb) for Ag ($Z=47$).

k/T_1 \ T_1	1 keV			5 keV			10 keV			50 keV			180 keV			500 keV		
	EC	ES	EBF	EC	ES	EBF	EC	ES	EBF	EC	ES	EBF	EC	ES	EBF	EC	ES	EBF
0.95		1.97	1.85		4.23	4.97		4.98	5.23		5.43	4.83		3.96	3.11	2.51	2.4[illegible]	[illegible]
0.80		1.90	1.91		4.17	5.12		5.01	5.45		5.74	5.20		4.49	3.62	3.19		
0.60		1.71	2.08		4.05	5.31		5.03	5.77		6.20	5.80				4.2[illegible]		
0.444														6.25	5.36			
0.40					3.89	5.45		5.03	6.11		6.83	6.57						
0.00		1.17	3.12		3.46	5.26		4.75	6.23		8.20	8.36		10.6	9.63		[illegible]	

TABLE V. Bremsstrahlung data $\beta_1^2(k/Z^2)(d\sigma/dk)$ (in mb) for Au ($Z=79$).

k/T_1 \ T_1	1 keV			5 keV			10 keV			50 keV			100 keV			500 keV		
	EC	ES	EBF	EC	ES	EBF	EC	ES	EBF	EC	ES	EBF	EC	ES	EBF	EC	ES	EBF
0.99					3.38	4.70				6.45	5.59	4.69				3.43	3.23	1.75
0.96										6.49	5.60	4.76					3.36	1.85
0.95		1.17	3.23															
0.90					3.40	4.77	6.41	4.30	5.11		5.67	4.90		5.59	4.20	3.83	3.62	2.07
0.80		1.15	3.18	6.24	3.31	4.84	6.50	4.26	5.24	6.78	5.79	5.14		5.80	4.50			
0.75																	4.27	2.69
0.60		0.94	3.11	6.46	3.11	4.97	6.73	4.16	5.51	7.26	6.06	5.71		6.31	5.21			
0.50																6.07	5.66	4.10
0.40					2.85	5.04	8.04	3.98	5.76	7.95	6.35	6.42						
0.00		0.55	2.71		2.23	4.68		3.42	5.73		7.18	7.85		8.90	8.62		11.47	9.89

TABLE VI. Bremsstrahlung data $\beta_1^2(k/Z^2)(d\sigma/dk)$ (mb) for U ($Z=92$).

T_1 / k/T_1	1 keV EC	1 keV ES	1 keV EBF	5 keV EC	5 keV ES	5 keV EBF	10 keV EC	10 keV ES	10 keV EBF	50 keV EC	50 keV ES	50 keV EBF	100 keV EC	100 keV ES	100 keV EBF	500 keV EC	500 keV ES	500 keV EBF
0.95		1.01	3.11		3.16	4.65		4.07	4.99		5.60	4.76		5.62	4.05		3.79	1.90
0.80		0.93	3.06		3.03	4.76		3.99	5.18		5.72	5.11		5.88	4.49		4.35	2.48
0.60		0.80	2.98		2.81	4.87		3.84	5.43		5.91	5.67		6.29	5.19		5.16	3.48
0.0		0.46	2.60		1.97	4.63		3.05	5.58		6.67	7.70		8.50	8.47		11.4	9.77

the coefficient $\frac{16}{3}\alpha^3$ of the $-\ln k$ term is precisely that obtained in a full (even relativistic) quantum mechanical treatment, as will be discussed subsequently, owing to the fact that the near-forward-angle behavior of the Rutherford cross section is the same in classical mechanics, nonrelativistic mechanics, and relativistic quantum mechanics.

The electron bremsstrahlung spectrum from a point Coulomb potential predicted in nonrelativistic quantum mechanics was obtained in dipole approximation by Sommerfeld[4] (which we designate S). The result is

$$\sigma(k)=\frac{16\pi^2}{3}\alpha^3\frac{1}{(e^{2\pi\nu_1}-1)(1-e^{-2\pi\nu_2})}X_0 \times\frac{d}{dX}\left|F(i\nu_1,i\nu_2;1;X_0)\right|^2 \tag{5}$$

with

$$\nu_i=Z\alpha/\beta_i \quad\text{and}\quad X_0=-4\nu_1\nu_2/(\nu_1-\nu_2)^2.$$

F is the hypergeometric function. Note that this depends on the three variables only in the two combinations ν_1 and ν_2. In the soft-photon limit $\nu_2\to\nu_1$ this reduces to Eq. (4) for all ν_1 up to constant terms. For low energies $\nu_1\gg 1$ and away from the soft-photon end of the spectrum, the Sommerfeld formula reduces[15] to the flat spectrum prediction Eq. (3). For high energies $2\pi\nu_1\ll 1$ and $2\pi\nu_2\ll 1$

TABLE VII. Other numerical bremsstrahlung data.

T_1 (keV)	k/T_1	$\beta_1^2\frac{k}{Z^2}\frac{d\sigma}{dk}$ (mb) $Z=2$	$Z=8$	$Z=13$	$Z=47$	$Z=79$
1	0.4	6.376				
5	0.2		7.355	6.501	3.642	2.484
	0.1					2.309
10	0.2		7.951		4.932	3.683
	0.1			7.626		3.492
50	0.2			8.29	7.504	6.80
	0.15		8.99			
	0.1			9.37		6.98
	0.05					7.12
	0.02					7.17
100	0.2		7.966	7.966		7.663
140	0.5					6.56
	0.143					8.56
180	0.98					4.76
	0.6					6.03
	0.3				7.30	
	0.2				8.20	
500	0.3			5.485		7.268
	0.2		6.473			7.416
	0.1			7.723		
1840	0.9978				1.35	1.93
	0.99				1.41	2.00
	0.98				1.47	2.07

TABLE VIII. Comparison for Al ($Z=13$).

		$\beta_1^2 \frac{k}{Z^2} \frac{d\sigma}{dk}$ (Coul.)									$\beta_1^2 \frac{k}{Z^2} \frac{d\sigma}{dk}$ (Kohn-Sham)						
T_1		S		B		EH		EB		EC	BF		EHF		EBF		ES
(keV)	k/T_1	mb	S/EC	mb	B/EC	mb	EH/EC	mb	EB/EC	mb	mb	BF/ES	mb	EHF/ES	mb	EBF/ES	mb
5	0.9	6.22	0.994	1.99	0.318	6.15	0.984	6.17	0.987	6.25	1.73	0.310	5.41	0.970	5.37	0.963	5.58
	0.8	6.41	0.994	2.93	0.454	6.36	0.986	6.43	0.996	6.45	2.53	0.444	5.56	0.975	5.54	0.971	5.70
	0.6	6.92	0.989	4.55	0.650	6.89	0.984	7.08	1.01	7.00	3.81	0.637	5.92	0.989	5.93	0.991	5.98
	0.5	7.27	0.987	5.39	0.732	7.25	0.985	7.51	1.02	7.36	4.40	0.718	6.12	0.999	6.12	0.999	6.13
	0.4	7.71	0.987	6.32	0.809	7.71	0.987	8.05	1.03	7.81	4.93	0.787	6.32	1.01	6.29	1.004	6.27
	0.2	9.20	0.983	8.87	0.947	9.26	0.989	9.84	1.05	9.36	5.79	0.894	6.63	1.02	6.43	0.989	6.50
	0.0	∞	1	∞	1	∞	1	∞	1	∞	6.28	0.974	6.28	0.974	6.28	0.974	6.63
50	0.9	4.18	1.004	1.75	0.420	4.02	0.964	4.03	0.967	4.17	1.73	0.418	3.97	0.959	3.98	0.961	4.14
	0.8	4.50	0.988	2.61	0.572	4.39	0.963	4.42	0.969	4.56	2.55	0.569	4.32	0.965	4.34	0.969	4.48
	0.6	5.31	0.957	4.13	0.744	5.36	0.966	5.40	0.973	5.55	4.00	0.738	5.19	0.958	5.22	0.963	5.42
	0.4	6.40	0.933	5.88	0.857	6.68	0.974	6.73	0.981	6.86	5.52	0.838	6.30	0.956	6.34	0.962	6.59
	0.2	8.19	0.903	8.44	0.929	8.84	0.974	8.93	0.984	9.08	7.51	0.906	7.89	0.952	7.94	0.958	8.29
	0.1	9.94	0.888	10.8	0.964	10.9	0.973	11.0	0.982	11.2	8.70	0.928	8.90	0.950	8.92	0.952	9.37
	0.0	∞	1	∞	1	∞	1	∞	1	∞	9.60	0.932	9.60	0.932	9.60	0.932	10.3
500	0.9	1.14	0.770	1.02	0.688	1.38	0.931	1.39	0.938	1.48	1.02	0.693	1.38	0.938	1.39	0.944	1.47
	0.75	1.56	0.669	1.93	0.824	2.19	0.937	2.20	0.941	2.34	1.92	0.825	2.18	0.937	2.19	0.943	2.33
	0.5	2.25	0.550	3.71	0.908	3.88	0.949	3.90	0.954	4.09	3.66	0.904	3.83	0.946	3.85	0.951	4.05
	0.0	∞	1	∞	1	∞	1	∞	1	∞	10.9	0.916	10.9	0.916	10.9	0.916	11.9

TABLE IX. Comparison for Au ($Z=79$).

		$\beta_1^2\frac{k}{Z^2}\frac{d\sigma}{dk}$ (Coul.)									$\beta_1^2\frac{k}{Z^2}\frac{d\sigma}{dk}$ (Kohn-Sham)						
T_1		S		B		EH		EB		EC	BF		EHF		EBF		ES
(keV)	k/T_1	mb	S/EC	mb	B/EC	mb	EH/EC	mb	EB/EC	mb	mb	BF/ES	mb	EHF/ES	mb	EBF/ES	mb
5	0.99										0.459	0.136	4.38	1.30	4.56	1.35	3.38
	0.9										1.48	0.435	4.60	1.35	4.64	1.37	3.40
	0.8	5.99	0.960	2.93	0.469	5.82	0.933	6.52	1.04	6.24	2.13	0.643	4.73	1.43	4.73	1.43	3.31
	0.6	6.19	0.958	4.55	0.704	6.05	0.936	7.17	1.15	6.46	3.09	0.993	4.93	1.58	4.87	1.56	3.11
	0.4										3.82	1.34	5.12	1.80	4.92	1.73	2.85
	0.2	7.22	0.963	8.87	1.18	7.17	0.956	9.90	1.32	7.50	4.33	1.74	5.36	2.16	4.84	1.95	2.48
	0.1										4.49	1.94	5.45	2.36	4.73	2.05	2.31
	0.0	∞	1	∞	1	∞	1	∞	1	∞	4.57	2.05	4.57	2.05	4.57	2.05	2.23
50	0.99	5.37	0.833	0.530	0.082	4.60	0.713	4.95	0.767	6.45	0.496	0.089			4.63	0.828	5.59
	0.9										1.62	0.286	4.47	0.788	4.83	0.852	5.67
	0.8	5.61	0.828	2.61	0.385	4.96	0.732	5.51	0.813	6.78	2.40	0.415	4.65	0.803	5.07	0.876	5.79
	0.6	5.95	0.820	4.14	0.570	5.48	0.754	6.27	0.864	7.26	3.71	0.612	5.11	0.843	5.64	0.931	6.06
	0.4	6.49	0.816	5.87	0.740	6.27	0.789	7.37	0.927	7.95	5.03	0.791	5.72	0.901	6.32	0.995	6.35
	0.2	7.54	0.810	8.44	0.906	7.70	0.828	9.31	1.001	9.30	6.50	0.957	6.64	0.976	7.17	1.05	6.80
	0.1	8.82	0.816	10.8	1.00	9.32	0.863	11.3	1.05	10.8	7.23	1.04	7.32	1.05	7.57	1.08	6.98
	0.05	10.2	0.836	12.8	1.06	11.1	0.902	13.1	1.07	12.3							
	0.0	∞	1	∞	1	∞	1	∞	1	∞	7.66	1.06	7.66	1.06	7.66	1.06	7.18
500	0.99	2.19	0.639	0.289	0.084	1.58	0.461	1.77	0.515	3.43	0.282	0.087	1.55	0.480	1.73	0.535	3.23
	0.9	2.26	0.589	1.02	0.266	1.85	0.483	2.10	0.548	3.83	0.990	0.273	1.80	0.497	2.05	0.565	3.62
	0.5	2.75	0.452	3.71	0.611	3.74	0.616	4.29	0.706	6.07	3.51	0.620	3.58	0.632	4.06	0.718	5.66
	0.0	∞	1	∞	1	∞	1	∞	1	∞	9.67	0.843	9.67	0.843	9.67	0.843	11.47

(apart from the tip region) the result becomes

$$\sigma(k)=\frac{16}{3}\alpha^3\ln\left(\frac{p_1+p_2}{p_1-p_2}\right), \tag{6}$$

while for high energies at the tip one has

$$\sigma(k)=(64\pi/3)\alpha^3\nu_1. \tag{7}$$

At low energies the tip value has simply the flat spectrum value $(16\pi/3\sqrt{3})\alpha^3$; so we have the prediction that at higher energies the tip value becomes small with decreasing Z and for all Z it decreases with increasing energy. Further, as the tip values are decreasing with increasing energy while the soft-photon end of the spectrum is remaining unchanged, we see that the spectrum, flat at low energies, becomes increasingly steep at higher energies. All these features are seen in our data. When we compare our numerical data with exact numerical predictions from the Sommerfeld formula, we see that in this point Coulomb case the formula is good (to ~1–4%) at 5 keV and for low Z still fairly good at 50 keV. This shows that, as in the atomic photoeffect,[22] cancellation is occurring between higher multipole and relativistic corrections to the nonrelativistic dipole approximation. This does not occur for the angular distributions, and it fails for the spectrum as the energy increases.

Since higher multipoles and relativistic effects give contributions of similar magnitude, to improve on the Sommerfeld formula for the point Coulomb case requires a full relativistic calculation. However, it has only been possible to obtain relativistic results in analytic form for a few limiting cases, while our numerical data (EC) give the full result of this theory for the energy range 1–500 keV where the partial-wave series has been obtained and numerically summed. The best known relativistic result is the relativistic Born approximation (which we designate B) obtained by Bethe and Heither,[5] requiring $\nu_1\ll 1$, $v_2\ll 1$. In this approximation the spectrum becomes

$$\sigma(k)=\alpha^3\left\{\frac{4}{3}-2E_1E_2\frac{p_1^2+p_2^2}{p_1^2p_2^2}+\frac{\epsilon_1E_2}{p_1^3}+\frac{\epsilon_2E_1}{p_2^3}-\frac{\epsilon_1\epsilon_2}{p_1p_2}\right.$$
$$\left.+L\left[\frac{\alpha E_1E_2}{3p_1p_2}+\frac{k^2(E_1^2E_2^2+p_1^2p_2^2)}{p_1^3p_2^3}+\frac{k}{2p_1p_2}\left(\frac{E_1E_2+p_1^2}{p_1^3}\epsilon_1-\frac{E_1E_2+p_2^2}{p_2^3}\epsilon_2+\frac{2kE_1E_2}{p_2^2p_1^2}\right)\right]\right\}, \tag{8}$$

where

$$L=2\ln\left(\frac{E_1E_2+p_1p_2-1}{k}\right),\quad \epsilon_1=\ln\left(\frac{E_1+p_1}{E_1-p_1}\right),\quad \epsilon_2=\ln\left(\frac{E_2+p_2}{E_2-p_2}\right).$$

In the soft-photon limit this again reduces to Eq. (4), while for the tip (where the condition $\nu_2\ll 1$ does not hold) this formula vanishes. If both $\beta_1\ll 1$ and $\beta_2\ll 1$ while still $\nu_1,\nu_2\ll 1$, Eq. (8) reduces to the nonrelativistic Born result Eq. (6), which, as we noted, can be extracted from the Sommerfeld formula.[4] The relativistic Born approximation is generally unsatisfactory for the point Coulomb situations of concern in this paper, except that like all the other theories it does give the correct logarithmically divergent result for the soft-photon end of the spectrum. The Born approximation always fails for high Z, for which $Z\alpha=O(1)$ and hence the ν's are not small. It always fails in the tip region of the spectrum, for which β_2 is small and hence ν_2 is large. And it always fails for low energies, for which the β's are small and the ν's large—the failure occurs already for higher energies as Z increases. We see this general feature of the Born approximation in our tables, where (B) and (EC) data are close only in the soft-photon region of the spectrum. However we may notice that the (B) data is fairly good for the low-Z case at 500 keV, and for still higher energies we may expect that the Born approximation will do well for the point Coulomb low-Z situation except in the tip region of the spectrum.

Elwert[6] found a simple way to improve the relativistic-Born-approximation result. By comparing the Sommerfeld formula with the Born-approximation formula, he obtained from the Sommerfeld formula a factor (Elwert factor)

$$f_E(\nu_1\nu_2)=\frac{\nu_2}{\nu_1}\frac{1-e^{-2\pi\nu_1}}{1-e^{-2\pi\nu_2}}. \tag{9}$$

When the Born-approximation result is multiplied by this factor (we designate this Elwert-Born combination EB) a substantially improved result for the spectrum is obtained. We have discussed elsewhere[10] some of the reasons for the success of this approximation, offering an explanation in terms of the properties of the electron wave functions which enter into the integral for the bremsstrahlung matrix element. Here let us simply note that this prescription replaces the Born-approximation prediction of zero for the tip of the spectrum with a finite prediction correct to lowest order in $Z\alpha$, while leaving unchanged the (correct) Born-approx-

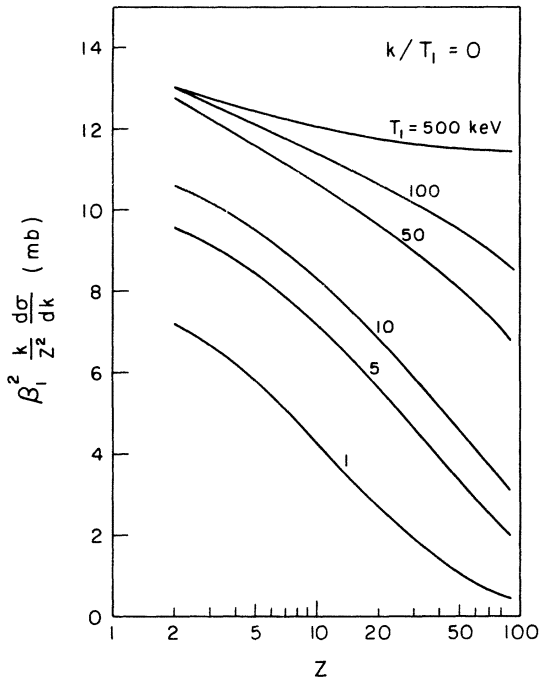

FIG. 1. Electron bremsstrahlung cross section $\sigma(k) \equiv \beta_1^2(k/Z^2)(d\sigma/dk)$ (in mb) at $k/T_1 = 0$ for $T_1 = 1-500$ keV and $Z = 2-79$, using the connection between elastic electron scattering and the low-frequency region of the bremsstrahlung spectrum.

imation prediction for the soft-photon end of the spectrum. In consequence we can expect a better result throughout the spectrum, particularly in the low-Z cases. This is what comparison of EB and EC data in our tables shows: for low Z, EB is good within several percent for all energies, while for high Z differences of a factor of 2 remain.

Under the circumstances that $T_1, T_2 \gg 1$, Bethe and Maximon[23] obtained an analytic expression for the relativistic point Coulomb bremsstrahlung spectrum, justifying and using Sommerfeld-Maue (SM)[24] wave functions for the calculation. It is believed that this calculation is only valid for $T_1 > 15-50$ MeV, far above the energies presently accessible in partial-wave calculations, and consequently there is no overlap with our discussion here. However more recently Elwert and Haug[7] used SM wave functions without high-energy assumptions to obtain a result (designated EH) for the spectrum which reduces to the Sommerfeld formula for low energies, to the Bethe-Maximon formula for high energies, and to the Bethe-Heither formula for low $Z\alpha/\beta$. Unfortunately, as our data show, at intermediate energies it gives predictions for the spectrum no better than those (EB) obtained from the Elwert-factor-multiplying Born approximation. (In the case of angular distributions it is more useful.)

Rather little can be said analytically about bremsstrahlung from a screened potential. The soft-photon end of the spectrum no longer diverges logarithmically but has a finite limit, because the total elastic scattering cross section is now finite. In the classical case at not too low an energy, this limit may be estimated from the Thomas-Fermi atomic model as[25]

$$\sigma(k) = \tfrac{16}{3}\alpha^3 \ln[\lambda(1.4/\alpha)(M\beta_1/Z^{1/3})], \tag{10}$$

where λ depends weakly on Z and T_1 and is of order of unity, and M is the mass of the atom. $\sigma(k)$ increases with $\ln T_1$ as T_1 increases and decreases as $-\ln Z$ as Z increases. We can see from Fig. 1 that for our energies, up to 100 keV, the data for the soft-photon limit in screened potentials does qualitatively exhibit these features.

In relativistic Born approximation the effect of screening is to multiply the cross-section differential in photon energy, photon angle, and scattered-electron angle by the square of a form factor

$$F(\vec{q}) = 1 - \frac{1}{Z}\int \rho(\vec{r}) e^{i\vec{q}\cdot\vec{r}}\, d\vec{r}, \tag{11}$$

where

$$\int \rho(\vec{r})\, d\vec{r} = Z, \tag{12}$$

with $\vec{q} = \vec{p}_1 - \vec{p}_2 - \vec{k}$. Here $\rho(\vec{r})$ is the charge density of the electron cloud, which is obtained in a self-consistent Hartree-Slater-type calculation.[12] To obtain the energy spectrum, the point Coulomb triply differential cross section weighted by $|F(\vec{q})|^2$

TABLE X. Integrated energy loss $\phi_{\rm rad}$.

	$\phi_{\rm rad}/Z^2\alpha^3\lambda_e^2$											
T_1	$Z=79$						$Z=13$					
(keV)	EC	B	EB	ES	BF	EBF	EC	B	EB	ES	BF	EBF
500	7.62	5.51	6.18	7.22	4.64	5.28	5.64	5.51	5.74	5.54	5.01	5.26
50	7.51	5.25	6.93	5.68	3.98	5.52	6.40	5.25	6.27	5.75	4.52	5.52
10	6.54	5.33	7.29	3.48	3.25	4.75	6.99	5.33	7.08	5.76	3.93	5.53

TABLE XI. Interpolated bremsstrahlung spectrum $\beta_1^2(k/Z^2)(d\sigma/dk)$ (mb) and integrated energy loss $\phi_{rad}/Z^2\alpha^3\lambda\!\!\!^{-2}_e$.

T_1 (keV) \ k/T_1	0.000	0.100	0.200	0.300	0.400	0.500	0.600	0.700	0.800	0.900	1.000	$\frac{\phi_{rad}}{Z^2\alpha^3\lambda\!\!\!^{-2}_e}$
						He ($Z=2$)						
1	7.147	7.315	7.197	6.916	6.546	6.146	5.758	5.413	5.136	4.962	4.980	5.309
2.5	8.513	8.466	8.009	7.419	6.792	6.177	5.594	5.045	4.527	4.045	3.726	5.383
5	9.555	9.233	8.419	7.572	6.779	6.049	5.369	4.723	4.091	3.448	2.866	5.371
10	10.606	9.860	8.634	7.558	6.641	5.834	5.099	4.402	3.710	2.973	2.133	5.327
25	11.912	10.321	8.576	7.284	6.273	5.427	4.675	3.968	3.257	2.473	1.377	5.205
50	12.804	10.580	8.554	7.137	6.055	5.164	4.382	3.656	2.935	2.145	0.968	5.189
75	12.955	10.439	8.339	6.902	5.812	4.919	4.141	3.422	2.714	1.944	0.779	5.109
100	13.029	10.294	8.144	6.693	5.602	4.713	3.942	3.235	2.543	1.796	0.663	5.046
200	13.079	9.869	7.602	6.114	5.025	4.154	3.410	2.742	2.103	1.433	0.440	4.922
300	13.042	9.642	7.316	5.800	4.708	3.849	3.120	2.475	1.869	1.246	0.346	4.922
400	13.014	9.528	7.170	5.629	4.533	3.677	2.959	2.327	1.738	1.141	0.296	4.987
500	13.002	9.477	7.105	5.540	4.439	3.581	2.871	2.247	1.667	1.083	0.268	5.088
						O ($Z=8$)						
1	4.821	4.988	5.082	5.112	5.103	5.067	5.016	4.960	4.908	4.868	4.848	4.315
2.5	6.414	6.580	6.605	6.559	6.467	6.342	6.193	6.026	5.839	5.631	5.398	5.379
5	7.615	7.715	7.549	7.298	7.015	6.728	6.452	6.188	5.938	5.702	5.470	5.824
10	8.739	8.683	8.178	7.601	7.047	6.548	6.115	5.748	5.454	5.247	5.151	5.889
25	10.113	9.646	8.609	7.649	6.821	6.112	5.510	5.000	4.577	4.251	4.128	5.770
50	10.959	10.097	8.733	7.586	6.622	5.797	5.083	4.459	3.907	3.411	3.071	5.663
75	11.364	10.131	8.560	7.317	6.302	5.445	4.707	4.059	3.475	2.926	2.468	5.514
100	11.598	10.079	8.372	7.072	6.033	5.165	4.420	3.765	3.170	2.597	2.062	5.399
200	11.975	9.765	7.781	6.380	5.314	4.450	3.715	3.070	2.477	1.891	1.237	5.155
300	12.097	9.541	7.437	5.992	4.924	4.073	3.353	2.722	2.141	1.566	0.891	5.091
400	12.159	9.403	7.240	5.769	4.703	3.861	3.153	2.531	1.958	1.391	0.712	5.115
500	12.202	9.321	7.130	5.640	4.577	3.740	3.042	2.427	1.856	1.291	0.607	5.185
						Al ($Z=13$)						
1	3.618	3.683	3.745	3.795	3.844	3.894	3.947	4.002	4.059	4.117	4.176	3.367
2.5	5.310	5.371	5.377	5.361	5.336	5.304	5.267	5.222	5.166	5.092	4.993	4.555
5	6.632	6.678	6.573	6.429	6.272	6.120	5.977	5.842	5.708	5.567	5.411	5.308
10	7.797	7.804	7.503	7.148	6.803	6.493	6.225	5.998	5.807	5.650	5.517	5.761
25	9.310	8.901	8.100	7.386	6.793	6.301	5.887	5.535	5.237	4.997	4.823	5.850
50	10.299	9.485	8.306	7.355	6.589	5.952	5.404	4.923	4.495	4.128	3.882	5.754
75	10.769	9.705	8.334	7.264	6.406	5.685	5.059	4.503	4.000	3.551	3.240	5.668
100	11.055	9.753	8.236	7.085	6.171	5.410	4.752	4.169	3.641	3.160	2.812	5.569
200	11.552	9.708	7.899	6.581	5.560	4.721	4.002	3.372	2.801	2.265	1.805	5.371
300	11.737	9.652	7.720	6.320	5.247	4.372	3.625	2.974	2.390	1.840	1.325	5.352
400	11.839	9.639	7.649	6.195	5.088	4.187	3.421	2.757	2.163	1.607	1.060	5.421
500	11.910	9.657	7.642	6.150	5.018	4.094	3.315	2.638	2.034	1.471	0.901	5.536
						Fe ($Z=26$)						
1	2.114	2.142	2.198	2.268	2.352	2.452	2.564	2.685	2.807	2.920	3.012	2.155
2.5	3.626	3.631	3.647	3.674	3.716	3.773	3.839	3.911	3.982	4.043	4.082	3.293
5	4.998	4.995	4.953	4.912	4.881	4.861	4.852	4.850	4.845	4.828	4.784	4.238
10	6.240	6.287	6.191	6.074	5.961	5.862	5.774	5.686	5.584	5.452	5.276	5.111
25	7.989	7.686	7.205	6.818	6.532	6.322	6.152	5.982	5.775	5.499	5.134	5.704
50	9.248	8.555	7.675	7.016	6.534	6.168	5.869	5.595	5.316	5.008	4.649	5.842
75	9.867	9.055	8.009	7.218	6.612	6.119	5.691	5.294	4.905	4.516	4.122	5.938
100	10.258	9.273	8.074	7.174	6.478	5.908	5.415	4.968	4.549	4.155	3.791	5.920
200	10.998	9.661	8.151	6.999	6.081	5.312	4.645	4.059	3.540	3.088	2.742	5.859
300	11.298	9.868	8.241	6.953	5.902	5.012	4.237	3.568	2.988	2.492	2.122	5.919
400	11.466	10.050	8.383	7.004	5.857	4.872	4.020	3.292	2.670	2.143	1.748	6.063
500	11.577	10.226	8.563	7.117	5.892	4.826	3.912	3.135	2.481	1.929	1.510	6.256
						Kr ($Z=36$)						
1	1.607	1.696	1.792	1.888	1.982	2.076	2.169	2.257	2.337	2.404	2.453	1.782
2.5	2.860	2.960	3.062	3.161	3.264	3.367	3.468	3.558	3.629	3.669	3.666	2.890

TABLE XI *(Continued)*

T_1 (keV) \ k/T_1	0.000	0.100	0.200	0.300	0.400	0.500	0.600	0.700	0.800	0.900	1.000	$\frac{\phi_{rad}}{Z^2\alpha^3\lambda_e^2}$
5	4.114	4.217	4.286	4.346	4.405	4.464	4.519	4.566	4.595	4.593	4.546	3.845
10	5.429	5.571	5.579	5.548	5.500	5.452	5.408	5.366	5.323	5.270	5.197	4.736
25	7.310	7.351	7.089	6.796	6.523	6.286	6.083	5.907	5.748	5.601	5.457	5.637
50	8.746	8.538	7.931	7.374	6.902	6.504	6.165	5.873	5.618	5.392	5.186	6.078
75	9.520	9.075	8.226	7.503	6.906	6.406	5.980	5.615	5.299	5.025	4.785	6.196
100	9.975	9.331	8.316	7.486	6.811	6.246	5.763	5.346	4.984	4.672	4.399	6.216
200	10.882	9.593	8.147	7.055	6.203	5.505	4.911	4.398	3.950	3.562	3.237	6.058
300	11.239	9.568	7.908	6.689	5.762	5.013	4.376	3.826	3.341	2.914	2.561	5.951
400	11.425	9.513	7.735	6.443	5.478	4.704	4.051	3.485	2.980	2.528	2.153	5.925
500	11.535	9.463	7.619	6.282	5.296	4.508	3.850	3.277	2.761	2.290	1.896	5.952
					Mo ($Z=42$)							
1	1.347	1.421	1.508	1.601	1.697	1.797	1.898	1.994	2.078	2.141	2.173	1.546
2.5	2.508	2.606	2.712	2.820	2.933	3.050	3.166	3.272	3.357	3.408	3.410	2.620
5	3.728	3.840	3.927	4.008	4.089	4.170	4.248	4.317	4.366	4.382	4.351	3.590
10	5.034	5.183	5.222	5.227	5.218	5.205	5.193	5.180	5.159	5.120	5.053	4.511
25	6.957	7.036	6.837	6.598	6.371	6.170	5.996	5.844	5.705	5.572	5.438	5.510
50	8.469	8.324	7.794	7.296	6.869	6.508	6.199	5.931	5.694	5.479	5.281	6.051
75	9.297	8.919	8.146	7.482	6.931	6.471	6.078	5.739	5.442	5.179	4.940	6.225
100	9.790	9.220	8.282	7.509	6.881	6.355	5.905	5.514	5.168	4.861	4.581	6.286
200	10.789	9.573	8.187	7.141	6.326	5.660	5.093	4.602	4.170	3.788	3.451	6.187
300	11.187	9.578	7.966	6.783	5.885	5.162	4.548	4.018	3.548	3.131	2.768	6.089
400	11.391	9.532	7.795	6.533	5.591	4.840	4.207	3.659	3.170	2.731	2.352	6.061
500	11.509	9.484	7.675	6.364	5.399	4.631	3.992	3.437	2.937	2.481	2.087	6.083
					Ag ($Z=47$)							
1	1.172	1.235	1.314	1.403	1.499	1.601	1.707	1.808	1.895	1.955	1.973	1.381
2.5	2.262	2.357	2.464	2.576	2.695	2.820	2.946	3.062	3.157	3.214	3.216	2.425
5	3.452	3.571	3.670	3.764	3.859	3.954	4.047	4.129	4.191	4.220	4.198	3.403
10	4.743	4.897	4.956	4.986	5.003	5.015	5.027	5.034	5.028	4.998	4.934	4.340
25	6.690	6.793	6.635	6.435	6.240	6.067	5.916	5.783	5.660	5.539	5.414	5.403
50	8.258	8.151	7.673	7.218	6.825	6.491	6.206	5.957	5.735	5.532	5.340	6.017
75	9.125	8.787	8.067	7.445	6.931	6.502	6.136	5.818	5.536	5.280	5.042	6.233
100	9.650	9.123	8.237	7.507	6.915	6.422	5.999	5.628	5.295	4.990	4.703	6.326
200	10.722	9.552	8.212	7.200	6.415	5.776	5.231	4.757	4.336	3.955	3.606	6.282
300	11.152	9.590	8.015	6.860	5.985	5.282	4.686	4.170	3.710	3.297	2.926	6.199
400	11.372	9.561	7.855	6.615	5.692	4.956	4.337	3.801	3.323	2.891	2.506	6.176
500	11.497	9.520	7.741	6.448	5.497	4.741	4.114	3.570	3.081	2.635	2.238	6.200
					La ($Z=57$)							
1	0.905	0.949	1.013	1.091	1.183	1.286	1.397	1.506	1.596	1.648	1.642	1.118
2.5	1.864	1.953	2.059	2.173	2.299	2.435	2.573	2.704	2.811	2.874	2.873	2.098
5	2.992	3.123	3.242	3.355	3.471	3.586	3.698	3.800	3.879	3.923	3.917	3.082
10	4.243	4.404	4.494	4.561	4.620	4.674	4.723	4.762	4.780	4.763	4.697	4.032
25	6.217	6.349	6.254	6.117	5.978	5.853	5.746	5.650	5.559	5.463	5.355	5.194
50	7.876	7.817	7.419	7.035	6.702	6.421	6.183	5.974	5.785	5.606	5.428	5.927
75	8.806	8.516	7.878	7.331	6.885	6.518	6.208	5.935	5.684	5.441	5.197	6.216
100	9.393	8.913	8.108	7.453	6.930	6.501	6.135	5.808	5.503	5.203	4.899	6.364
200	10.604	9.501	8.236	7.289	6.563	5.976	5.477	5.037	4.634	4.251	3.875	6.444
300	11.099	9.624	8.120	7.016	6.182	5.517	4.951	4.459	4.015	3.604	3.213	6.413
400	11.350	9.647	8.009	6.809	5.913	5.201	4.601	4.082	3.618	3.193	2.798	6.418
500	11.489	9.642	7.928	6.666	5.732	4.988	4.372	3.840	3.364	2.931	2.532	6.461
					W ($Z=74$)							
1	0.601	0.612	0.648	0.707	0.787	0.890	1.013	1.140	1.243	1.273	1.202	0.797
2.5	1.379	1.443	1.533	1.643	1.774	1.924	2.086	2.241	2.363	2.414	2.365	1.670
5	2.411	2.556	2.696	2.833	2.972	3.111	3.242	3.359	3.446	3.489	3.472	2.659
10	3.573	3.728	3.847	3.960	4.075	4.188	4.292	4.372	4.408	4.377	4.256	3.589
25	5.570	5.698	5.658	5.591	5.526	5.475	5.439	5.410	5.376	5.323	5.236	4.853

TABLE XI *(Continued)*

T_1 (keV) \ k/T_1	0.000	0.100	0.200	0.300	0.400	0.500	0.600	0.700	0.800	0.900	1.000	$\frac{\phi_{rad}}{Z^2\alpha^3\lambda_e^2}$
50	7.352	7.274	6.941	6.641	6.400	6.215	6.071	5.950	5.832	5.697	5.527	5.734
75	8.350	7.996	7.424	6.982	6.663	6.431	6.251	6.086	5.899	5.657	5.332	6.108
100	9.032	8.456	7.702	7.152	6.763	6.482	6.258	6.048	5.808	5.497	5.093	6.319
200	10.454	9.346	8.163	7.323	6.714	6.247	5.854	5.491	5.117	4.700	4.221	6.654
300	11.057	9.746	8.365	7.348	6.583	5.971	5.446	4.976	4.533	4.094	3.644	6.814
400	11.365	10.006	8.532	7.395	6.511	5.785	5.162	4.619	4.135	3.695	3.287	6.978
500	11.534	10.206	8.698	7.474	6.496	5.675	4.979	4.382	3.872	3.437	3.072	7.161
					Au ($Z=79$)							
1	0.552	0.571	0.610	0.667	0.741	0.834	0.942	1.054	1.146	1.184	1.140	0.743
2.5	1.283	1.356	1.450	1.559	1.685	1.826	1.975	2.120	2.237	2.299	2.277	1.583
5	2.274	2.425	2.570	2.709	2.847	2.984	3.115	3.231	3.323	3.379	3.384	2.552
10	3.412	3.580	3.709	3.829	3.946	4.059	4.163	4.246	4.292	4.279	4.190	3.479
25	5.378	5.526	5.510	5.463	5.413	5.375	5.348	5.328	5.304	5.264	5.194	4.757
50	7.167	7.126	6.830	6.557	6.334	6.163	6.030	5.920	5.814	5.694	5.543	5.677
75	8.188	7.893	7.364	6.949	6.643	6.419	6.245	6.088	5.915	5.695	5.401	6.087
100	8.894	8.385	7.675	7.147	6.770	6.494	6.275	6.074	5.849	5.564	5.193	6.324
200	10.379	9.329	8.182	7.360	6.763	6.304	5.920	5.571	5.215	4.820	4.367	6.709
300	11.014	9.734	8.379	7.381	6.632	6.037	5.529	5.078	4.654	4.232	3.796	6.883
400	11.337	9.980	8.524	7.409	6.549	5.849	5.251	4.731	4.266	3.840	3.438	7.046
500	11.510	10.158	8.661	7.463	6.518	5.732	5.068	4.499	4.008	3.585	3.220	7.222
					Rn ($Z=86$)							
1	0.496	0.528	0.572	0.629	0.695	0.773	0.859	0.947	1.024	1.073	1.074	0.681
2.5	1.168	1.256	1.357	1.465	1.582	1.707	1.837	1.963	2.073	2.150	2.177	1.477
5	2.102	2.261	2.411	2.551	2.688	2.820	2.946	3.061	3.159	3.235	3.278	2.413
10	3.208	3.396	3.540	3.666	3.782	3.890	3.988	4.071	4.129	4.150	4.121	3.337
25	5.117	5.297	5.315	5.295	5.264	5.238	5.220	5.208	5.195	5.172	5.130	4.626
50	6.902	6.925	6.687	6.450	6.250	6.091	5.966	5.864	5.770	5.672	5.556	5.594
75	7.952	7.767	7.310	6.928	6.632	6.405	6.226	6.070	5.913	5.733	5.510	6.061
100	8.690	8.309	7.673	7.175	6.800	6.515	6.286	6.084	5.879	5.644	5.357	6.335
200	10.260	9.318	8.225	7.423	6.829	6.369	5.988	5.652	5.327	4.984	4.602	6.780
300	10.938	9.696	8.370	7.395	6.665	6.092	5.610	5.191	4.804	4.424	4.030	6.954
400	11.279	9.885	8.437	7.352	6.533	5.880	5.332	4.860	4.438	4.043	3.657	7.094
500	11.459	9.996	8.488	7.329	6.448	5.736	5.145	4.639	4.194	3.794	3.422	7.237
					U ($Z=92$)							
1	0.457	0.501	0.553	0.609	0.669	0.733	0.799	0.866	0.931	0.988	1.034	0.639
2.5	1.084	1.187	1.295	1.403	1.511	1.622	1.732	1.840	1.942	2.033	2.108	1.398
5	1.970	2.135	2.289	2.430	2.563	2.690	2.809	2.922	3.026	3.119	3.201	2.304
10	3.049	3.257	3.414	3.544	3.656	3.754	3.843	3.922	3.991	4.046	4.083	3.224
25	4.901	5.111	5.160	5.161	5.144	5.124	5.109	5.100	5.094	5.087	5.072	4.515
50	6.670	6.758	6.573	6.368	6.184	6.030	5.906	5.804	5.718	5.639	5.558	5.521
75	7.743	7.675	7.289	6.935	6.638	6.397	6.199	6.033	5.888	5.752	5.617	6.040
100	8.503	8.266	7.706	7.230	6.846	6.537	6.284	6.069	5.880	5.702	5.525	6.349
200	10.144	9.318	8.278	7.488	6.886	6.412	6.022	5.691	5.397	5.120	4.842	6.837
300	10.857	9.641	8.337	7.376	6.661	6.104	5.646	5.259	4.914	4.587	4.256	6.991
400	11.213	9.749	8.296	7.234	6.455	5.853	5.359	4.944	4.573	4.218	3.854	7.091
500	11.396	9.773	8.237	7.114	6.300	5.669	5.162	4.733	4.347	3.975	3.588	7.189

must be integrated (generally numerically) over angles. (We have designated this Born approximation with form factor BF.) Note that since $|F|<1$ screening, as in the classical case, decreases the cross section. In an *ad hoc* fashion, one can also modify the EH and EB triply differential cross section by the same form factor and integrate over angles, obtaining the spectrum predictions designated EHF and EBF in our tables. These predictions all show the property of a finite soft-photon spectrum limit, corresponding to the fact that the Born approximation for elastic scattering from a

screened potential is finite. BF still suffers from vanishing at the tip limit (which the exact result does not do unless one looks within 10 eV of the tip); EHF and EBF gave rather similar results. From its origin in Born approximation we might anticipate that a form factor best assesses screening for low-Z elements, and this is what our data show; the fractional change in a spectrum point due to screening is well predicted for low Z and poorly predicted for high Z. At these energies the importance of screening diminishes with increasing energy, as the important region for the process moves into the interior of the atom. At much higher energies this situation is known to reverse and screening again becomes important. We note that throughout the energy range of interest EBF is within a factor of 2 of ES for high-Z elements and within a few percent for low-Z elements.

Finally in Table X we compare predictions for the integrated bremsstrahlung energy-loss cross section $\phi_{\rm rad}$, defined as[26]

$$\phi_{\rm rad} = \frac{1}{E_1}\int^{T_1} k\frac{d\alpha}{dk}\,dk\,. \tag{13}$$

In the integration one sees a tendency for Coulomb increases in the tip region to cancel screening decreases in the soft-photon region, so that integrated B, EBF, and ES points lie between more extreme EC and BF points. In low-Z elements B and EBF lie within ~5–10% of our numerical ES data, while in the high-Z case the discrepancies range from 20% (500 keV) to 70% (10 keV). Thus, here too none of the simple approximations are generally acceptable for quantitative purposes.

IV. TABULATION OF THE BREMSSTRAHLUNG ENERGY SPECTRUM FROM NEUTRAL ATOMS

We can now develop an interpolation scheme for tabulation of the bremsstrahlung spectrum. As mentioned in Sec. II, the factor $k\beta_1^2/Z^2$ serves to scale $d\sigma/dk$. However, we can see from Tables I–VI that for a fixed Z and T_1 the variation of the bremsstrahlung cross section $\sigma(k)\equiv\beta_1^2(k/Z^2)(d\sigma/dk)$ over a spectrum can be a factor of 10, especially for low-Z elements and high energies. In Sec. III we have observed that for incident electron kinetic energies above 1 keV, by combining the Bethe-Heitler formula, the Elwert factor, and a form factor one comes within a factor of 2 of the exact numerical screened results for high-Z elements and within a few percent for low-Z elements. Thus the ratios $\sigma_{\rm EBF}/\sigma_{\rm ES}$ vary very smoothly with respect to the three variables Z, T_1, and k/T_1. This provides the basis of an interpolation scheme for the bremsstrahlung spectrum from neutral atoms.

In Tables I–VI, we have given the "benchmark" data for six elements at various incident electron kinetic energies $T_1 = 1$–500 keV. For fixed Z and fixed T_1, we use the following interpolation formula

$$\sigma_{\rm EBF}(k)/\sigma_{\rm ES}(k) = a_1 + a_2 y + a_3 y^2 + a_4 y^3 \tag{14}$$

with $y = k/T_1$. With this formula and the data presented in Tables I–VI, we can construct the entire spectrum for all the cases presented in Tables I–VI, accurate to within about 2%. To enlarge these tabulations, for fixed k/T_1 we use the Lagrange three-point interpolation formula in Z and $\ln T_1$ for the ratios $\sigma_{\rm EBF}/\sigma_{\rm ES}$ to interpolate in Z and $\ln T_1$. There are two orders in which this can be done. The results from these two different orders agreed to better than 0.1%. However, if the interpolation is performed in a completely different order (not beginning with k/T_1), the results can vary by as much as 5%. Conservatively, we believe that our interpolated values are accurate to at least 10%.

In Table XI we present a short tabulation of the bremsstrahlung spectrum $\sigma(k)$ for neutral atoms

TABLE XII. Comparison of interpolated bremsstrahlung spectrum $[\beta_1^2(k/Z^2)(d\sigma/dk)$ (in mb)] with experimental results.

	$Z=13$				$Z=79$					
T_1	50 keV		500 keV		50 keV		180 keV		500 keV	
k/T	Calc.	Expt. (Ref. 29)[a]	Calc.	Expt. (Ref. 28)	Calc.	Expt. (Ref. 29)	Calc.	Expt. (Ref. 27)	Calc.	Expt. (Ref. 28)
0.90	4.13	3.81 ± 0.34	1.47	2.01 ± 0.37	5.69	5.52 ± 0.34			3.59	5.50 ± 1.20
0.80	4.50	4.26 ± 0.31	2.03	2.90 ± 0.75	5.81	5.81 ± 0.34	5.35	4.67 ± 0.54	4.01	5.96 ± 1.20
0.60	5.40	5.31 ± 0.41	3.12	4.09 ± 0.90	6.03	6.32 ± 0.43	6.01	5.26 ± 0.54	5.07	7.00 ± 1.50
0.40	6.59	6.35 ± 0.60	5.02	5.88 ± 1.10	6.33	7.15 ± 0.51	6.79	5.94 ± 0.72	6.52	8.15 ± 1.60
0.25							7.70	6.62 ± 0.82		
0.20	8.31	7.82 ± 0.60								
0.15							8.63	7.16 ± 1.00		

[a] All the experimental results were read from the figures in the references.

obtained with this interpolation scheme, for incident electron kinetic energies $T_1 = 1-500$ keV and elements $Z = 2-79$. The results are estimated to be accurate within 10%.[27] We will subsequently prepare more extensive tables of these results.

Finally, in Table XII we compare our predicted results with existing recent experimental data[28-30] for the spectrum. The agreement achieved seems generally satisfactory when the combined experimental and theoretical uncertainties are considered.

---

*Supported in part by the Department of Health, Education, and Welfare under Grant FD 00653-02 and in part by the National Science Foundation under Grant MPS 74-03531 A01.

[1]H. K. Tseng and R. H. Pratt, Phys. Rev. A 1, 528 (1970).
[2]For example, D. G. Brown, U. S. Department of Health, Education and Welfare Report No. BRH/DEP 70-18, 1970 (unpublished).
[3]For example, S. Von Goeler, W. Stodiek, H. Eubank, H. Fishman, S. Grebenshchikov, and E. Hinnov, Nucl. Fusion 15, 301 (1975).
[4]A. Sommerfeld, Ann. Phys. (Leipz.) 11, 257 (1931).
[5]H. A. Bethe and W. Heitler, Proc. R. Soc. Lond. A 146, 83 (1934); F. Sauter, Ann. Phys. (Leipz.) 20, 404 (1934); G. Racah, Nuovo Cimento 11, 461 (1934); 11, 467 (1934).
[6]G. Elwert, Ann. Phys. (Leipz.) 34, 178 (1939).
[7]G. Elwert and E. Haug, Phys. Rev. 183, 90 (1969).
[8]H. W. Koch and J. W. Motz, Rev. Mod. Phys. 31, 920 (1959).
[9]H. K. Tseng and R. H. Pratt, Phys. Rev. Lett. 33, 516 (1974).
[10]R. H. Pratt and H. K. Tseng, Phys. Rev. A 11, 1797 (1975).
[11]C. M. Lee and R. H. Pratt, Phys. Rev. A 12, 707 (1975).
[12]D. A. Liberman, D. T. Cromer, and J. T. Waber, Comput. Phys. Commun. 2, 107 (1971); W. Kohn and L. J. Sham, Phys. Rev. 140, A1133 (1965).
[13]G. Molière, Z. Naturforsch. 2a, 133 (1947).
[14]F. E. Low, Phys. Rev. 110, 974 (1958); T. H. Barnett and N. M. Kroll, Phys. Rev. Lett. 20, 86 (1968); I. S. Brown and R. T. Gable, Phys. Rev. 173, 1505 (1968).
[15]For example, I. I. Sobelman, *Introduction to the Theory of Atomic Spectra* (Pergamon, New York, 1972), p. 374.
[16]C. M. Lee, R. H. Pratt, L. Kissel, and H. K. Tseng, *Abstracts of Papers of the Ninth International Conference on the Physics of Electronic and Atomic Collision*, edited by J. S. Risley and R. Geballe (University of Washington Press, Seattle, 1975), p. 406.
[17]U. Fano, Phys. Rev. 116, 1156 (1959).
[18]C. M. Lee and R. H. Pratt, Phys. Rev. A 12, 1825 (1975).
[19]C. M. Lee, S. Yu, and R. H. Pratt (unpublished).
[20]S. R. Lin, Phys. Rev. 133, A965 (1964).
[21]For example, L. D. Landau and E. M. Lifshitz, *The Classical Theory of Fields*, 3rd ed. (Pergamon, New York, 1971), p. 69 and 70.
[22]J. McEnnan, S. D. Oh, and R. H. Pratt (unpublished).
[23]H. A. Bethe and L. C. Maximon, Phys. Rev. 93, 768 (1954).
[24]A. Sommerfeld and A. W. Maue, Ann. Phys. (Leipz.) 22, 629 (1935).
[25]For example, J. D. Jackson, *Classical Electrodynamics* (Wiley, New York, 1962), Chap. 15.
[26]W. Heitler, *The Quantum Theory of Radiation* (Oxford U.P., London, 1954), 3rd ed., p. 242.
[27]We may note that the numerical data of Table VII, not used because it was believed not to be of reference standard accuracy, turns out to agree with the interpolated values within 5% except for 500 keV, where the number of partial waves used was inadequate.
[28]G. Klasmeier, dissertation (University of Würzburg, 1962) (unpublished).
[29]J. W. Motz, Phys. Rev. 100, 1560 (1955).
[30]J. W. Motz and R. C. Placious, Phys. Rev. 109, 235 (1958).